ENVIRONMENTAL RESEARCH
LETTERS

LETTER • OPEN ACCESS

Urban vegetation cooling potential during heatwaves depends on background climate

To cite this article: Jiacheng Zhao *et al* 2023 *Environ. Res. Lett.* **18** 014035

IOP Publishing Environ. Res. Lett. 18 (2023) 014035 https://doi.org/10.1088/1748-9326/acaf0f

ENVIRONMENTAL RESEARCH
LETTERS

OPEN ACCESS

RECEIVED
23 September 2022

REVISED
15 December 2022

ACCEPTED FOR PUBLICATION
29 December 2022

PUBLISHED
12 January 2023

LETTER

Urban vegetation cooling potential during heatwaves depends on background climate

Jiacheng Zhao[1,2,3], **Naika Meili**[3], **Xiang Zhao**[1,2,*] **and Simone Fatichi**[3]

[1] State Key Laboratory of Remote Sensing Science, Jointly Sponsored by Beijing Normal University and Aerospace Information Research Institute of Chinese Academy of Sciences, Faculty of Geographical Science, Beijing Normal University, Beijing 100875, People's Republic of China
[2] Beijing Engineering Research Center for Global Land Remote Sensing Products, Institute of Remote Sensing Science and Engineering, Faculty of Geographical Science, Beijing Normal University, Beijing 100875, People's Republic of China
[3] Department of Civil and Environmental Engineering, National University of Singapore, Singapore 117576, Singapore
[*] Author to whom any correspondence should be addressed.

E-mail: zhaoxiang@bnu.edu.cn

Keywords: urban vegetation, heatwave, cooling potential, stomatal behavior

Supplementary material for this article is available online

Abstract

The capacity of vegetation to mitigate excessive urban heat has been well documented. However, the cooling potential provided by urban vegetation during heatwaves is less known even though heatwaves have been projected to be more severe with climate change. Across 24 global metropolises, we combine 30 m resolution satellite observations with a theoretical leaf energy balance model to quantify the change of the leaf-to-air temperature difference and stomatal conductance during heatwaves from 2000 to 2020. We found the responses of urban vegetation to heatwaves differ significantly across cities and they are mediated by climate forcing and human management. During heatwaves, vegetation in Mediterranean and midlatitude-humid cities shows a significant decrease in cooling potential in most cases due to large stomatal closures, while vegetation in arid cities shows a cooling enhancement with an unmodified stomatal opening likely in response to intense irrigation. In comparison, the cooling potential of vegetation in high-latitude humid cities does not show significant changes. These responses have implications for future urban vegetation management strategies and urban planning.

1. Introduction

Heatwaves have been observed to increase both in frequency and severity due to climate change (Skinner *et al* 2018, Perkins-Kirkpatrick and Lewis 2020). Nearly one-third of the world's population is currently exposed to deadly heat for at least 20 d per year and an increasing number of people are likely to experience such climatic conditions in the future under all emission scenarios (Mora *et al* 2017). For people living in urban areas, the threat of this impending heat stress is greater due to localized synergies of heatwaves and urban heat islands (UHIs) in different climates and urban development patterns (Li and Bou-Zeid 2013, Wouters *et al* 2017, Khan *et al* 2020, He *et al* 2021). The case in metropolises could be even worse because of the positive relationship between the level of heat stress and population density (Luo and Lau 2018, Zander *et al* 2018).

An often-proposed mitigation strategy to counteract extreme urban heat is the increase of vegetation in cities (Gaffin *et al* 2012, Wong *et al* 2021). It has been well-documented that vegetation reduces the local temperature in multiple ways such as by providing shade and transpiration, which replaces sensible heat with latent heat (Gunawardena *et al* 2017, Lai *et al* 2019, Meili *et al* 2021). However, how urban vegetation behaves during heatwaves when its cooling is most needed is uncertain but crucial for vegetation survival and its ecological benefits in cities. During heatwaves, raised temperature and vapor pressure deficit (VPD) typically increase transpirative demand but induce stomatal closure to avoid water loss, which in turn restrains transpirative cooling (Grossiord *et al*

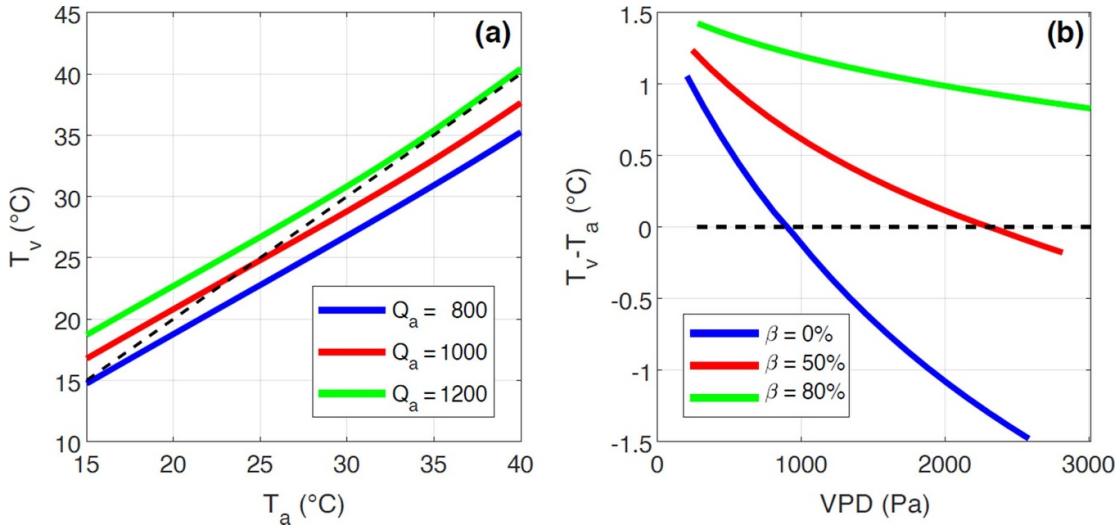

Figure 1. Example simulation of (a) the relationships between T_v and T_a for one single leaf receiving different levels of radiation (Q_a) and (b) how $T_v - T_a$ changes with VPD under different levels of water stress, where $\beta = 0\%$ indicates the leaf is well-watered and $\beta = 50\%$ and 80% represent the level of stomatal closure when compared to a well-watered leaf. When not specified $Q_a = 1000$ W m^{-2}, $T_a = 25$ °C, relative humidity = 65%, wind speed = 1.5 m s^{-1}, atmospheric CO_2 concentration = 400 ppm and atmospheric pressure = 1013 hPa. The dashed black line in (a) is the 1:1 standard line.

2020, Kimm *et al* 2020). This is even more the case when the heatwave coincides with a drought that largely decreases soil moisture (He *et al* 2022). However, for urban vegetation, irrigation can potentially maintain evapotranspiration elevated and therefore enhance the cooling potential (Gao and Santamouris 2019, Gao *et al* 2020). An opposite behavior was also observed in some species showing that plants open or retain their stomatal opening if they receive irrigation or can access water with deep roots (Drake *et al* 2018, Aparecido *et al* 2020). A glasshouse experiment in Australasia indicates that this is the case for plants with inherently low stomatal conductance (g_s) and which typically experience droughts because they are likely to be at a higher risk of heat-related leaf damage and therefore, need transpiration to reduce their leaf temperature (Marchin *et al* 2022). In the US, satellite-based evidence also shows a prevalent enhanced cooling capacity of urban trees during heatwaves (Wang *et al* 2019) but the magnitude of such enhancements varies across cities. Thus, whether plants provide more or less cooling during heatwaves and the magnitude of cooling they provide are uncertain and they will depend on the environmental conditions (soil moisture, VPD, wind speed, etc) and the extent to which plants adjust their stomatal opening. All these factors vary geographically and therefore require a more extensive investigation across cities in a wide range of climates.

Vegetation regulates its leaf canopy temperature (T_v) through transpiration to maintain functional biochemical and physiological processes (TESKEY *et al* 2015, Muller *et al* 2021). Depending on leaf traits and the leaf atmospheric coupling, T_v can be higher or lower than air temperature (T_a) (Leuzinger *et al* 2010, Feng and Zou 2019). The leaf-to-air temperature difference ($T_v - T_a$) is a key variable describing vegetation cooling potential that affects the sensible heat flux between plant surfaces and the air (Moran *et al* 1994, Muller *et al* 2021) and changes with meteorological conditions. $T_v - T_a$ can be computed by concurrently solving leaf photosynthesis, g_s, and the energy balance for a given leaf or a canopy. In the following, we show an example of how climatic and environmental conditions such as available radiation, VPD and water availability can influence the relationship between T_v and T_a using a mechanistic modeling approach (Bonan 2019) (figure 1). In the given example, a well-watered leaf receiving a moderate amount of radiation ($Q_a = 1000$ W m^{-2}), where Q_a is the sum of net shortwave radiation and incoming longwave radiation, has a theoretically higher T_v than T_a when T_a is lower than 25 °C, above which T_v becomes lower than T_a and the leaf starts cooling the ambient air (figure 1(a)). However, when Q_a increases to 1200 W m^{-2}, the transpirative cooling cannot offset the radiative warming and higher T_v than T_a is observed across all analyzed T_a values. The opposite occurs at $Q_a = 800$ W m^{-2}. All else being equal, $T_v - T_a$ significantly decreases (more cooling) as VPD increases but the rate of the decrease can be notably suppressed by water stress which limits g_s (figure 1(b)). Although theoretically these mechanisms are well described and can be used to evaluate vegetation's cooling potential (i.e. $T_v - T_a$ in this study), measuring them in real conditions is challenging, and little is known about how heatwaves modify $T_v - T_a$ of urban plants in different cities and climates, especially considering contrasting stomatal responses.

To quantitatively derive the cooling potential and stomatal behavior of urban vegetation, we used 30 m satellite-retrieved land surface temperatures (LSTs) and meteorological variables from the ERA5-Land reanalysis product to compute $T_v - T_a$ during heatwave periods since 2000 across 24 global cities located in climates ranging from humid to semi-arid to arid (figure S1). The value of $T_v - T_a$ is used to infer g_s by inverting a theoretical formulation of the canopy energy budget and to answer the questions: do urban plants close or open their stomata during heatwaves in comparison to normal climatic conditions? Is there a correlation between stomatal behavior and city background climate? Addressing these questions can shed light on the potential of vegetation to provide cooling during heatwaves, when it is likely most needed, and concurrently guide urban greening strategies.

2. Data and methods

Heatwave days in this study are defined as five or more consecutive with a maximum T_a above its 90th percentile in the city during summer (from June to early September) for the period 2000–2020 (figure S2). Normal summer days are defined as the remaining summer days during this period. Days with daily precipitation of more than 2 mm were excluded to remove effects associated with recent rainfall and interception. To analyze the response of urban vegetation to heatwaves, we selected several typical urban green spaces (UGSs) that are present from 2000 to 2020 and are fully covered by vegetation in each city. Most UGSs are fully covered by trees while UGSs in a few arid cities are covered by grasses mixed with trees. The boundaries of the UGSs are determined using multiple datasets including the 10 m European Space Agency (ESA) WorldCover, the 30 m National Land Cover Database (Yang *et al* 2018), the long-term global land-cover product with fine classification system at 30 m (GLC_FCS30) (Zhang *et al* 2021), and high-resolution google historical images. The 30 m Landsat thermal images (from all of Landsat 5, Landsat 7 and Landsat 8) were used to retrieve the LST (T_v) of these UGSs and the 9 km ERA5-Land hourly reanalysis product (globally available at hourly scale since 1981) (https://cds.climate.copernicus.eu/#!/home) was used to extract the 2 m air temperature (T_a) that is spatially and temporally matched to each of the T_v observations to calculate $T_v - T_a$. Other meteorological variables used in this study are also extracted from the ERA5-Land hourly product. More details on the selection criteria of UGSs and description of the T_v and T_a data are provided in supporting information S1.

Note, while there is a mismatch in the spatial resolution between the two data sets, the spatial heterogeneity of T_a in urban areas is generally much smaller than that of T_v (Eliasson 1990). For example, data from urban weather stations in Shenzhen show that within-city daytime LSTs ranging from 25 °C to 40 °C only result in a T_a spatial variability of 30 °C–31.5 °C (Cao *et al* 2021). A comparison of the ERA5-Land Hourly T_a values with a high-resolution (100 m) simulation product of T_a generated for European cities with the urban climate model Urb-Clim (Hooyberghs *et al* 2019) shows that the maximum difference of T_a at 11:00 a.m. local time, which is close to the Landsat overpass times (∼10:30 a.m. local time), on one typical summer day in Paris is less than 1 °C (figure S3). Furthermore, throughout July 2015, there is a high correlation between T_a at different resolutions in vegetated areas ($R^2 = 0.93$, figure S4) for a humid city (Paris) and semi-arid city (Madrid), selected as examples.

A single leaf absorbs incoming solar radiation $R_{sw}^{\downarrow}$ and long-wave radiation $L^{\downarrow}$ from the atmosphere and surrounding surfaces and emits long-wave radiation $L^{\uparrow}$ as a function of its leaf temperature. The net absorbed radiation is then partitioned into sensible heat H and latent heat λE according to the energy balance as follows

$$R_{sw}^{\downarrow}(1-\alpha) + L^{\downarrow} - L^{\uparrow} = H + \lambda E \tag{1}$$

where α is the surface albedo. $L^{\uparrow} = \varepsilon_v \sigma T_v^4$ where ε_v is the leaf emissivity and $\sigma = 5.67 \times 10^{-8}$ is the Stefan–Boltzmann constant. $H = \rho_a C_p \frac{T_v - T_a}{r_b/2 + r_a}$ where ρ_a is the air density, C_p is the specific heat capacity of the air, r_b is the leaf boundary layer resistance and r_a is the aerodynamic resistance. $\lambda E = \frac{\rho_a C_p}{\gamma} \frac{(e_{sat}(T_v) - e_a)}{r_s + r_b + r_a}$ where $\gamma \approx 67$ is the psychrometric constant, r_s is the stomatal resistance, e_{sat} is the saturation vapor pressure and e_a is the actual vapor pressure. Equation (1) can be rewritten as

$$Q_a - \varepsilon_v \sigma T_v^4 = \frac{\rho_a C_p (T_v - T_a)}{\frac{1}{2g_b} + \frac{1}{g_a}} + \frac{\rho_a C_p}{\gamma} \frac{(e_{sat}(T_v) - e_a)}{\frac{1}{g_s} + \frac{1}{g_b} + \frac{1}{g_a}} \tag{2}$$

where Q_a is the total available energy for the leaf which is the sum of absorbed solar radiation and incoming long-wave radiation, $g_b = 1/r_b$ is the boundary layer conductance, $g_a = 1/r_a$ is the aerodynamic conductance, and $g_s = 1/r_s$ is the stomatal conductance. Here g_b and g_a follow the parameterization as used in the Urban Tethys-Chloris (UT&C) model (Meili *et al* 2020). A more detailed description of the calculation of g_b and g_a is provided in supporting information S2.

Since remotely sensed T_v measures the vegetation canopy temperature rather than the temperature of a single leaf, it is necessary to upscale g_b and g_s from the leaf to the canopy scale. This is done by simply multiplying the conductance g_b and g_s by the leaf area index (LAI), which was calculated by an artificial

neural network trained on a radiative transfer model (PROSAIL) inversion that can predict LAI from the Landsat surface reflectances (Martínez-Ferrer *et al* 2022). Then, equation (2) becomes

$$Q_a - \varepsilon_v \sigma T_v^4 = \frac{\rho_a C_p (T_v - T_a)}{\frac{1}{2LAIg_b} + \frac{1}{g_a}} + \frac{\rho_a C_p}{\gamma} \frac{(e_{sat}(T_v) - e_a)}{\frac{g_s + g_b}{LAIg_b g_s} + \frac{1}{g_a}} \tag{3}$$

$$Q_a - \varepsilon_v \sigma T_v^4 = 2LAIg_b g_a \frac{\rho_a C_p (T_v - T_a)}{g_a + 2LAIg_b} + LAIg_b g_s g_a \frac{\rho_a C_p}{\gamma} \frac{(e_{sat}(T_v) - e_a)}{g_a g_s + g_a g_b + LAIg_b g_s}. \tag{4}$$

Equation (4) is non-linear in T_v. To obtain an analytical solution, we use a Taylor's expansion to approximate T_v around T_a, which gives $T_v^4 \approx T_a^4 + 4T_a^3(T_v - T_a)$ and $e_{sat}(T_v) - e_a \approx e_{sat}(T_a) + \Delta(T_v - T_a) - e_a$ where Δ is the slope of e_{sat} computed at T_a. With this we obtain

$$\begin{aligned} Q_A - \varepsilon_v \sigma \left(T_a^4 + 4T_a^3 (T_v - T_a)\right) &= 2LAIg_b g_a \frac{\rho_a C_p (T_v - T_a)}{g_a + 2LAIg_b} + LAIg_b g_s g_a \frac{\rho_a C_p}{\gamma} \\ &\times \frac{(e_{sat}(T_a) + \Delta(T_v - T_a) - e_a)}{g_a g_s + g_a g_b + LAIg_b g_s} \end{aligned} \tag{5}$$

which gives an analytical expression for $T_v - T_a$:

$$T_v - T_a = \left(Q_a - \varepsilon_v \sigma T_a^4 - \frac{1}{\gamma} \frac{LAIg_b g_s g_a \rho_a C_p VPD}{g_a g_s + g_a g_b + LAIg_b g_s}\right) \Big/ \left(4\varepsilon_v \sigma T_a^3 + \frac{2LAIg_b g_a \rho_a C_p}{g_a + 2LAIg_b} + \frac{1}{\gamma} \frac{LAIg_b g_s g_a \rho_a \Delta C_p}{g_a g_s + g_a g_b + LAIg_b g_s}\right). \tag{6}$$

For each observation of $T_v - T_a$, we numerically solve equation (6) to obtain the value of g_s that satisfies equation (6). All other terms in equation (6) are either measured (T_v, T_a, Q_a, VPD, etc) or calculated (g_b, g_a, etc), based on aerodynamic considerations. In this way, we approximate g_s during heatwaves and normal summer days over UGSs in the analyzed cities. All variables/parameters and their units used in this study are listed in table S1.

3. Results

We first compared the changes in meteorological variables during heatwaves and normal climatic conditions in all 24 selected cities (figure 2). By definition, T_a is statistically larger during heatwaves (figure 2(b)). We also found that VPD significantly ($p < 0.05$, t-test) increased on heatwave days compared to normal summer days in most cities (figure 2(d)). Additionally, half of the cities also showed significantly stronger solar radiation during heatwaves (figure 2(a)). T_a can exceed 40 °C for some arid cities such as Baghdad, Dubai and Phoenix with VPD exceeding 6 kPa. Seven cities showed a significantly decreased wind speed during heatwaves (figure 2(c)). Since heatwave durations in most cities are relatively short (less than 10 d, figure S5), UGSs only showed a slightly decreased greenness (indicated by normalized difference vegetation index, NDVI) and the decreases are only significant in Houston and Denver (figure 2(e)). A few cities showed a significant increase of NDVI (e.g. Wuhan and Shanghai), which might be related to modified radiative conditions. Despite the relatively consistent changes in meteorological variables, we observed distinct patterns of the leaf-to-air temperature difference $T_v - T_a$ (figure 2(f)), which in most conditions is a positive number, i.e. vegetation is warmer than the surrounding air. For several high-latitude humid cities including Baltimore, Moscow, London, Berlin, Oslo and Chicago, $T_v - T_a$ showed almost no change between heatwave and normal summer days, while for Mediterranean cities such as Madrid, Rome, Barcelona and Lisbon, $T_v - T_a$ increased (although not always statistically significant) on average by 0.8 °C–2.6 °C, when compared to $T_v - T_a$ on normal summer days. The increasing $T_v - T_a$ indicates that the cooling potential of plants in these cities decreased during heatwaves as sensible heat increases driven by the positive $T_v - T_a$. Some midlatitude humid cities such as Wuhan, Paris and Shanghai also showed an increased $T_v - T_a$. In contrast, the average $T_v - T_a$ decreased by 1.4 °C–4.8 °C in six arid cities (Baghdad, Dubai, Phoenix, Las Vegas, Abu Dhabi and Denver).

Within a given city, the response of urban vegetation to heatwaves is spatially consistent across UGSs (figure 3). For example, the $T_v - T_a$ of UGSs in Paris universally increased during heatwaves however with different magnitudes in various

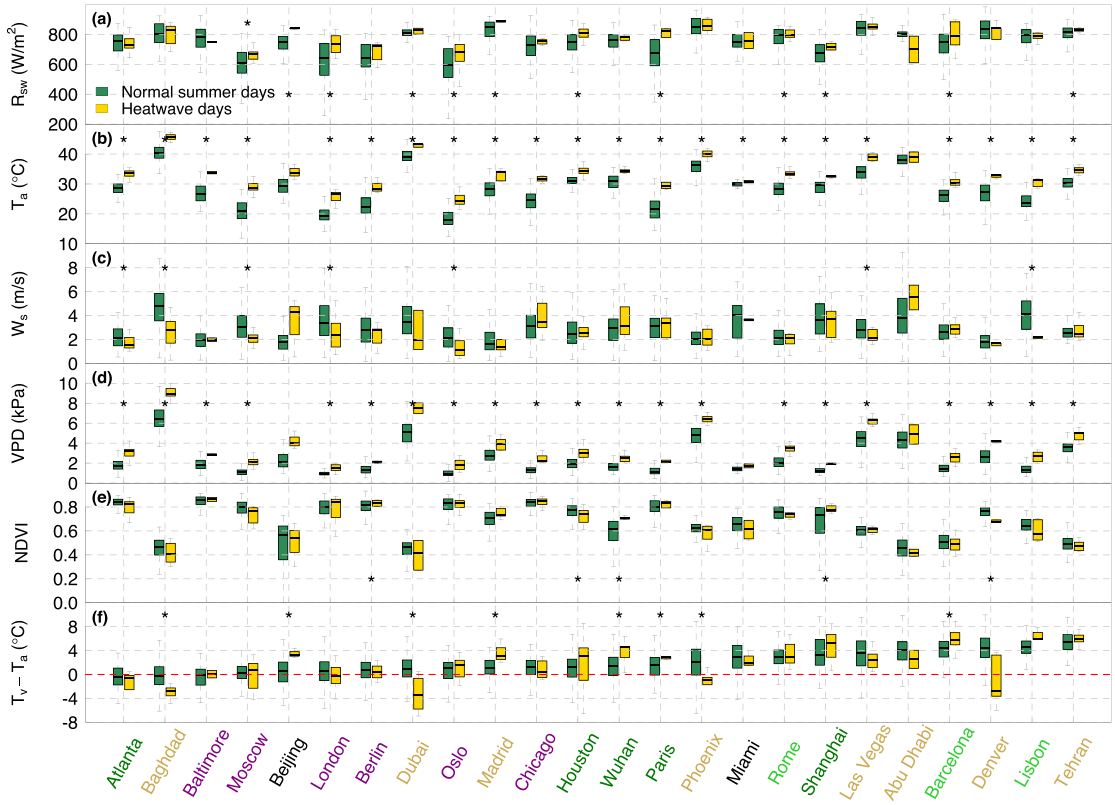

Figure 2. Comparison of meteorological variables, NDVI and $T_v - T_a$ between normal summer days (green box) and heatwave days (yellow box). The asterisk indicates that a significant ($p < 0.05$, t-test) difference exists between the mean value of the two groups. According to the Köppen–Geiger climate classification (figure S1), we group these cities into high-latitude humid cities (in purple), predominantly midlatitude humid cities (in dark green), Mediterranean cities (in light green), arid cities (in tan), and cities in other climates (in black).

UGSs (figures 3(a)–(c)). Small UGSs showed a higher increase in $T_v - T_a$ compared to larger UGSs and the T_v of small UGSs can be up to 10 °C higher than T_a on heatwave days in Paris (figure 3(c)). The effect of heatwaves was more pronounced in Madrid, where $T_v - T_a$ increased up to 20 °C for most grasslands, which are likely wilted or highly water-stressed and almost completely lose their cooling function (figures 3(d)–(f)). However, tree-covered UGSs in downtown Madrid were less affected by the heatwaves compared to the grasslands. This discrepancy is likely related to different rooting depths and also irrigation practices. In contrast to Paris and Madrid, all UGSs in Phoenix, which are mostly grasslands and irrigated, showed a consistently decreased $T_v - T_a$ during heatwaves (figures 3(g)–(i)).

To explain the different responses of $T_v - T_a$ to heatwaves across cities, we numerically computed the g_s for each observation of $T_v - T_a$ (figure 4). For the same value of g_s, $T_v - T_a$ is commonly lower during heatwaves than during normal summer days, indicating a higher cooling potential of vegetation in hotter and higher VPD conditions if plants are not water stressed, which is the case where plants are intensively irrigated in arid cities. In this case, results suggest that vegetation keeps its stomata relatively open during heatwaves (Baghdad, Abu Dhabi, Dubai, Las Vegas, Phoenix and Denver).

However, for Mediterranean cities experiencing a hot and dry summer such as Lisbon, Rome, Barcelona and Madrid, T_v on normal summer days was prevalently higher than T_a, resulting in a positive $T_v - T_a$ larger than 3 °C. This indicates that plants in these cities are already under water stress on normal summer days (figure 1(b)). Their g_s is generally between 0.2 and 0.3 mol H_2O m^2 s^{-1} (figure 5(a)). During heatwaves, the plants further close their stomata and therefore show a decreased g_s of around 0.15 mol H_2O m^2 s^{-1} (figure 5(b)) and raised $T_v - T_a$, which approaches 6 °C in some cities (figure 4).

For humid cities, plants also commonly closed their stomata and show a decreased g_s (although

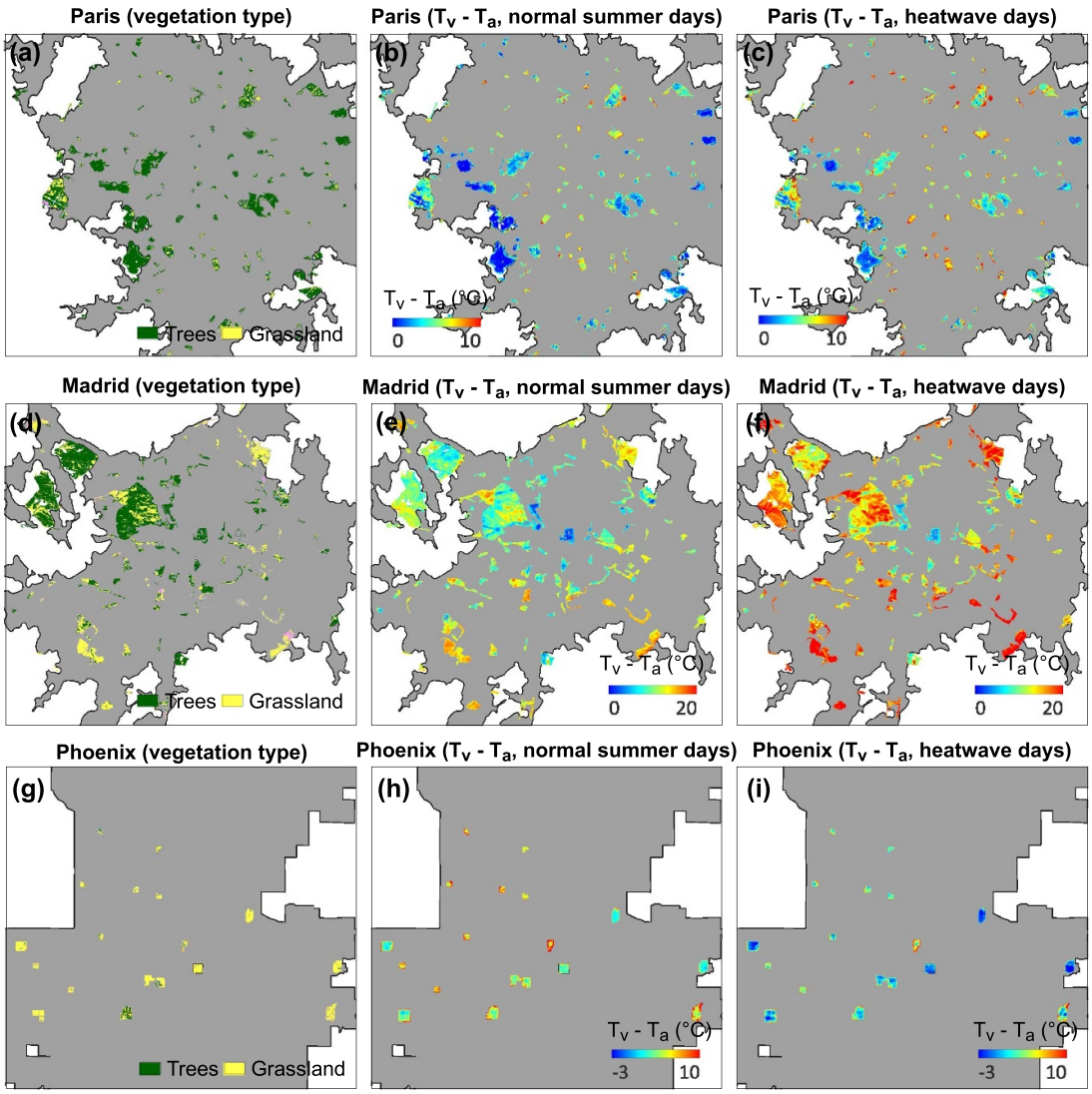

Figure 3. Spatial comparisons of $T_v - T_a$ between normal summer days and heatwave days for Paris, Madrid and Phoenix. The left column (a), (d), (g) shows the vegetation type as derived from the ESA WorldCover 10 m 2020 product. The middle (b), (e), (h) and right (c), (f), (i) columns show the average $T_v - T_a$ on normal summer days and heatwave days from June to early September during the period 2000–2020, respectively.

not always statistically significant) during heatwave days (figure 4). However, $T_v - T_a$ of high-latitude cities (London, Oslo, Berlin, Moscow, Chicago and Baltimore) showed no significant difference compared to normal summer days even when g_s significantly decreased (figures 2(f) and 4). Most midlatitude humid cities including Paris, Wuhan, Shanghai and Houston showed increases of $T_v - T_a$ ranging from 1.1 °C to 2.7 °C. We also found that $T_v - T_a$ is positively related to heatwave intensity (defined as the degree-hours that are the sum of hours with T_a above the 90th percentile of daily maximum T_a in the city during summer, weighted by the departure of hourly T_a from the 90th percentile) in a few cities (e.g. Moscow, Chicago, Wuhan, Houston, Atlanta, Baghdad, Las Vegas, Phoenix, figure S6) and thus an increase in $T_v - T_a$ is observed with increasing heatwave intensity. Meanwhile, g_s mostly follows the change of $T_v - T_a$ and shows a negative relationship with heatwave intensity in some cities leading to larger stomatal closure with higher intensity (figure S7).

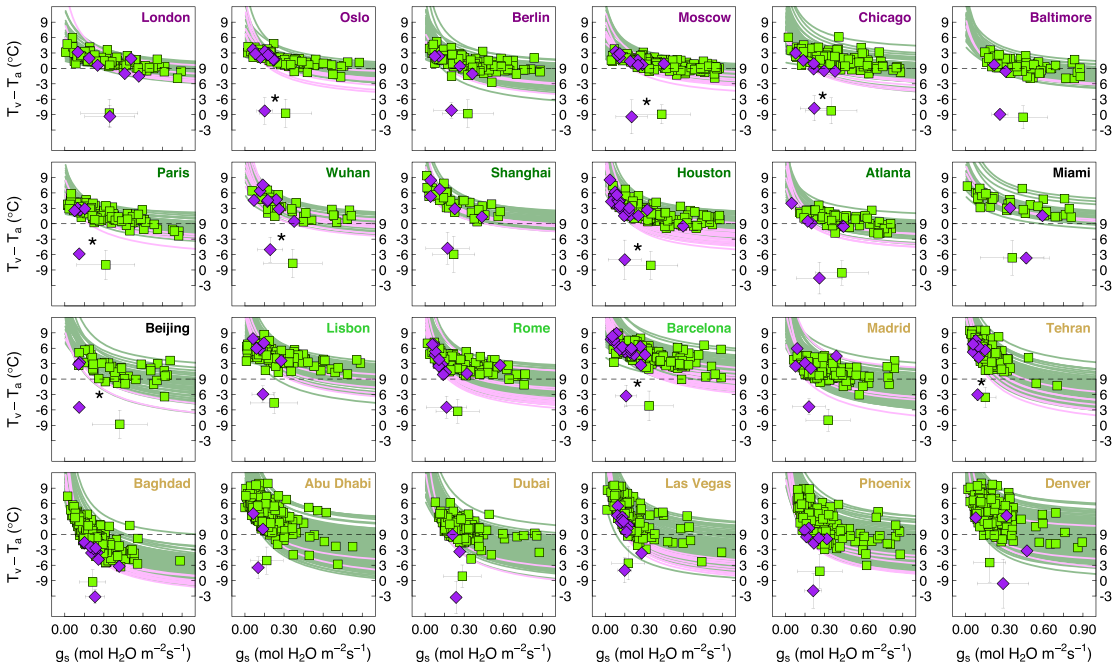

Figure 4. Stomatal conductance (g_s) during normal summer days and heatwave days. Each line indicates a theoretical relationship between $T_v - T_a$ and g_s at the daily scale (~10:30 a.m. local time) (green lines for normal summer days and pink lines for heatwave days). Dots indicate the observation of $T_v - T_a$ and the corresponding computed g_s (green ones for normal summer days and purple ones for heatwave days). $T_v - T_a$ and g_s of the two groups are statistically compared in the form of the box-and-whisker plot and the asterisk indicates that a significant ($p < 0.05$, t-test) difference exists between the mean g_s of the two groups. To avoid overlap over individual dots, these boxes were moved down by nine units (°C) and readers can check the secondary y-axis for specific values. According to the Köppen–Geiger climate classification (figure S1), we group these cities into high-latitude humid cities (in purple), predominantly midlatitude humid cities (in dark green), Mediterranean cities (in light green), arid cities (in tan), and cities in other climates (in black). The unit of g_s is converted from m s^{-1} to mol H_2O m^{-2} s^{-1} to be comparable with plant physiological literature (supporting information S3).

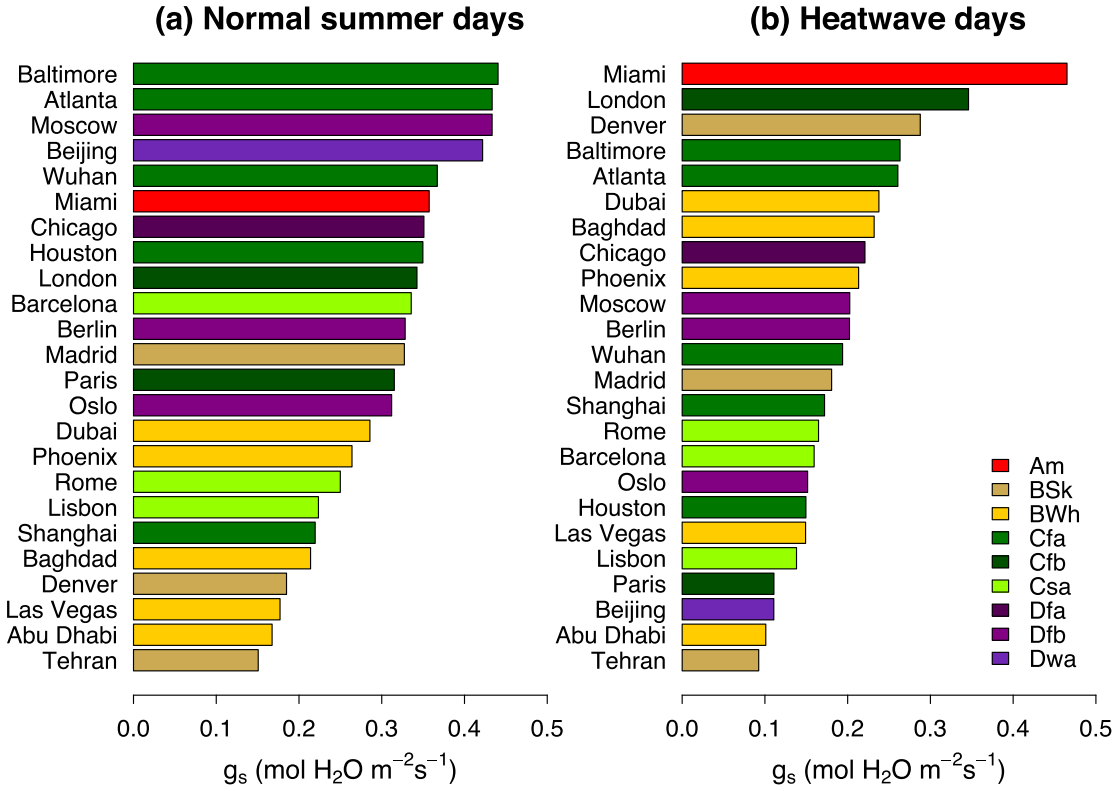

Figure 5. Ranking of the mean g_s in the 24 selected cities during normal summer days (a) and heatwave days (b). The colors of the bars represent the climate classification of the city as shown in figure S1.

4. Discussion and conclusion

We combined 30 m resolution satellite observations with a theoretical leaf energy balance model to analyze how urban vegetation responds to heatwave conditions across 24 global metropolises. Unavoidable uncertainties in LST from remote sensing observations (Cook 2014, Laraby 2017) and T_a from reanalysis (Hersbach *et al* 2020, Araújo *et al* 2022) are filtered by using a large number of time steps for each city and by fitting a theoretical $T_v - T_a$ vs. g_s model in each time step. Although T_a in cities experiencing strong UHIs is likely underestimated in the used dataset, the canopy T_a UHI is on average much smaller than the surface temperature UHI (Venter *et al* 2021), especially during daytime and it is unlikely to generate any major effect on the results. To quantify the potential impact of variations or uncertainty in T_a, we also tested the sensitivity of the g_s results to the variability in T_a by adding an error term to T_a for each observation. Even with a large error term of $\varepsilon \sim N$ (3 °C, 1 °C), that assumes a large uncertainty in T_a, results show that the $T_v - T_a$ and g_s response to heatwaves (i.e. how $T_v - T_a$ and g_s changes during heatwaves) in each city remain the same (figures 4 and S8). Hence, the changes of $T_v - T_a$ and g_s are robust at the city scale even without accounting for the within-city spatial heterogeneity of T_a.

Our results highlight that the response of urban vegetation has a geographical divergence which is largely related to background climate forcing and to vegetation management, i.e. irrigation. In high-latitude humid cities, there are no significant changes in the leaf-to-air temperature difference ($T_v - T_a$) (figures 2(f) and 4), which indicates that the vegetation cooling potential of these cities was not affected by the heatwave conditions. This is because of (a) similar g_s during normal summer days and heatwave days in some cities such as London (figure 4) and (b) relatively higher g_s (figure 5(a)) and overall less sensitivity of $T_v - T_a$ to higher g_s than to lower g_s (see the curvature change of the theoretical relationship between $T_v - T_a$ and g_s in figure 4). For instance, a significantly decreased g_s does not change $T_v - T_a$ in Moscow as lower g_s is likely compensated by changes in meteorological conditions (figures 2 and 4). However, in midlatitude humid cities such as Wuhan, Shanghai and Houston, we found significant stomatal closure which led to increased $T_v - T_a$ during heatwaves. Due to generally abundant summer rainfall in these cities, urban vegetation is mainly rainfed and expected to still provide substantial cooling even during heatwaves or extended dry periods when cooling is likely most needed. However, our results do not support this assumption and suggest that urban vegetation in such cities, with the current management strategies, provides less rather than more cooling under extreme heat conditions. This effect is even exacerbated in vegetation with lower canopy heights, which showed higher $T_v - T_a$ than that of vegetation with higher canopy heights for similar g_s (see an example in Houston, figure S9). This suggests that increased irrigation is likely needed to fulfill the water demand of urban vegetation and to maintain its cooling potential during heatwaves.

Vegetation in the Mediterranean is widely known for experiencing and being adapted to low water availability (Galmés *et al* 2007, Rana *et al* 2020). We found that heatwaves exacerbated plant water stress as stomatal closure is more pronounced than during normal conditions and such closure limits transpiration, which is originally already at low levels (figure 5). During heatwaves, as plants close stomata further, we observe a much higher T_v than T_a indicating that Mediterranean urban plants are actually unlikely to considerably cool urban air. However, plant T_v could be still lower than those of impervious surfaces and their exact cooling potential during heatwaves requires further investigation.

UGSs in arid cities, which are mostly covered by grasses, were found to retain stomatal opening during heatwaves at a similar level than during normal days. Given the higher atmospheric water demand, $T_v - T_a$ for a similar g_s shows lower values during heatwaves than normal summer days in arid climates (figure 4). This contrasts with the reduced green roof cooling potential during heatwave/drought conditions found in other studies (Speak *et al* 2013, Zhang *et al* 2020). However, by keeping stomata relatively open, these plants have a considerably enhanced cooling potential, which given the extremely high VPD, is counterintuitive, and not captured by most stomatal conductance models (Leuning 1995, Damour *et al* 2010, Medlyn *et al* 2011, Meili *et al* 2021) that will predict stomatal closure at such VPD levels independently from water availability (Yang *et al* 2019, Meili *et al* 2021). This result sheds light on the importance of watering vegetation during extreme weather conditions (Zhang *et al* 2020).

Regardless of heatwave conditions, $T_v - T_a$ generally follows the gradient of vegetation NDVI (figures 2(e) and (f)), i.e. dense and healthy UGSs lead to higher cooling potential. However, all our results combined show the critical role of stomatal behavior and background climate in the responses of the cooling potential to heatwaves (figure 4), especially given the remarkable difference of such responses, for example, in Phoenix and Barcelona with both having a decreased NDVI (figures 2(e) and (f)). A large decrease of g_s and stomatal closure during heatwaves can directly suppress plant transpiration and increase leaf temperature (T_v), which might prevent any transpirative cooling and puts plants at risk of lethal overheating if they fail to keep T_v below the leaf critical temperature, generally 46 °C–49 °C (Hüve *et al* 2011, O'sullivan *et al* 2017). Nevertheless, even in the dry Mediterranean cities experiencing severe water stress, plants close their stomata as these critical

temperatures are likely not reached even during heatwaves in these cities (figure 2(b)), or herbaceous vegetation is already wilted. Conversely, when plants have enough water available (in humid and irrigated cities) they keep stomata open even when atmospheric water demand is significant.

Our analysis has unavoidable limitations in terms of data and methodological choices. The rare occurrence of heatwaves and cloud contamination in some cities results in a limited number of observations during heatwave days and induces uncertainty in cooling potential and g_s estimation. The use of the first-order Taylor's expansion can also cause some bias in estimating g_s, especially when leaf temperature strongly deviates from air temperature. Beyond this, even though most UGSs chosen in this study are fully covered by trees, in a few arid cities (i.e. Abu Dhabi, Dubai, Las Vegas and Phoenix) UGSs are mainly covered by grasses and contain only a few trees, in which case our modeled g_s could have larger uncertainties. Irrigation on urban grasslands can strongly change soil moisture and can lead to evaporation from water intercepted on the grass leaves or from the soil underneath, which can make $T_v - T_a$ not representative of leaf temperature only. Compared to the low-frequency Landsat observations used here, future studies could focus on daily observations to quantify the change of stomatal behavior throughout the whole heatwave and potentially associated drought period.

In summary, we explore for one of the first times how $T_v - T_a$ and g_s, which are good proxies for the cooling potential of urban vegetation, respond to current heatwaves in different climates and cities. Results highlight the crucial role of human intervention through irrigation in all those climates where vegetation might undergo partial or substantial water stress. Mediterranean and midlatitude humid cities are shown to experience a significantly suppressed cooling potential as plants are mostly rainfed and they largely decrease g_s when cooling (transpiration) will be most needed (e.g. during heatwaves). However, cooling enhancement is observed in arid cities because irrigation is largely shifting the behavior of g_s leading to equal or higher g_s than on normal summer days. As a result, while urban greening is a desirable strategy to achieve multiple ecosystem services (Haase *et al* 2014, Richards *et al* 2022), its capability to reduce temperature during heatwaves might not match expectations derived from normal summer days and cannot be thought of disjointly from strategies to supply necessary water requirements. This is becoming even more relevant in a rapidly changing climate.

Data availability statements

All data that support the findings of this study are included within the article (and any supplementary files).

Acknowledgments

This study was funded by the National Natural Science Foundation of China (42090012). The authors thank the China Scholarship Council (202106040091) for funding the first author's (J Zhao) research attachment at National University of Singapore. N Meili and S Fatichi acknowledge the support of the National University of Singapore through the project 'Bridging scales from below: The role of heterogeneities in the global water and carbon budgets', Award No. 22-3637-A0001.

Conflict of interest

The authors declare no conflicts of interest relevant to this study.

ORCID iDs

Jiacheng Zhao https://orcid.org/0000-0002-1493-4723
Naika Meili https://orcid.org/0000-0001-6283-2134
Xiang Zhao https://orcid.org/0000-0002-0155-6735
Simone Fatichi https://orcid.org/0000-0003-1361-6659

References

Aparecido L M T, Woo S, Suazo C, Hultine K R and Blonder B 2020 High water use in desert plants exposed to extreme heat *Ecol. Lett.* **23** 1189–200

Araújo C S P D, Silva I A C E, Ippolito M and Almeida C D G C D 2022 Evaluation of air temperature estimated by ERA5-Land reanalysis using surface data in Pernambuco, Brazil *Environ. Monit. Assess.* **194** 381

Bonan G 2019 *Climate Change and Terrestrial Ecosystem Modeling* (Cambridge: Cambridge University Press)

Cao J, Zhou W, Zheng Z, Ren T and Wang W 2021 Within-city spatial and temporal heterogeneity of air temperature and its relationship with land surface temperature *Landsc. Urban Plan.* **206** 103979

Cook M J 2014 *Atmospheric compensation for a landsat land surface temperature product* (Rochester Institute of Technology) (available at: https://scholarworks.rit.edu/theses/8513)

Damour G, Simonneau T, Cochard H and Urban L 2010 An overview of models of stomatal conductance at the leaf level *Plant Cell Environ.* **33** 1419–38

Drake J E *et al* 2018 Trees tolerate an extreme heatwave via sustained transpirational cooling and increased leaf thermal tolerance *Glob. Change Biol.* **24** 2390–402

Eliasson I 1990 Urban geometry, surface temperature and air temperature *Energy Build.* **15** 141–5

Feng H and Zou B 2019 A greening world enhances the surface-air temperature difference *Sci. Total Environ.* **658** 385–94

Gaffin S R, Rosenzweig C and Kong A Y Y 2012 Adapting to climate change through urban green infrastructure *Nat. Clim. Change* **2** 704

Galmés J, Medrano H and Flexas J 2007 Photosynthetic limitations in response to water stress and recovery in Mediterranean plants with different growth forms *New Phytol.* **175** 81–93

Gao K and Santamouris M 2019 The use of water irrigation to mitigate ambient overheating in the built

environment: recent progress *Build. Environ.* **164** 106346
Gao K, Santamouris M and Feng J 2020 On the cooling potential of irrigation to mitigate urban heat island *Sci. Total Environ.* **740** 139754
Grossiord C, Buckley T N, Cernusak L A, Novick K A, Poulter B, Siegwolf R T W, Sperry J S and McDowell N G 2020 Plant responses to rising vapor pressure deficit *New Phytol.* **226** 1550–66
Gunawardena K R, Wells M J and Kershaw T 2017 Utilising green and bluespace to mitigate urban heat island intensity *Sci. Total Environ.* **584–5** 1040–55
Haase D *et al* 2014 A quantitative review of urban ecosystem service assessments: concepts, models, and implementation *Ambio* **43** 413–33
He B-J, Wang J, Liu H and Ulpiani G 2021 Localized synergies between heat waves and urban heat islands: implications on human thermal comfort and urban heat management *Environ. Res.* **193** 110584
He B-J, Wang J, Zhu J and Qi J 2022 Beating the urban heat: situation, background, impacts and the way forward in China *Renew. Sustain. Energy Rev.* **161** 112350
Hersbach H *et al* 2020 The ERA5 global reanalysis *Q. J. R. Meteorol. Soc.* **146** 1999–2049
Hooyberghs H, Berckmans J, Lauwaet D, Lefebre F and de Ridder K 2019 Climate variables for cities in Europe from 2008 to 2017, version 1.0 (available at: https://cds.climate.copernicus.eu/cdsapp#!/dataset/sis-urban-climate-cities?tab=overview)
Hüve K, Bichele I, Rasulov B and Niinemets Ü 2011 When it is too hot for photosynthesis: heat-induced instability of photosynthesis in relation to respiratory burst, cell permeability changes and H_2O_2 formation *Plant Cell Environ.* **34** 113–26
Khan H S, Paolini R, Santamouris M and Caccetta P 2020 Exploring the synergies between urban overheating and heatwaves (HWs) in western Sydney *Energies* **13** 470
Kimm H, Guan K, Gentine P, Wu J, Bernacchi C J, Sulman B N, Griffis T J and Lin C 2020 Redefining droughts for the U.S. corn belt: the dominant role of atmospheric vapor pressure deficit over soil moisture in regulating stomatal behavior of maize and soybean *Agric. For. Meteorol.* **287** 107930
Lai D, Liu W, Gan T, Liu K and Chen Q 2019 A review of mitigating strategies to improve the thermal environment and thermal comfort in urban outdoor spaces *Sci. Total Environ.* **661** 337–53
Laraby K 2017 *Landsat surface temperature product: global validation and uncertainty estimation* (Rochester Institute of Technology)
Leuning R 1995 A critical appraisal of a combined stomatal-photosynthesis model for C_3 plants *Plant Cell Environ.* **18** 339–55
Leuzinger S, Vogt R and Körner C 2010 Tree surface temperature in an urban environment *Agric. For. Meteorol.* **150** 56–62
Li D and Bou-Zeid E 2013 Synergistic interactions between urban heat islands and heat waves: the impact in cities is larger than the sum of its parts *J. Appl. Meteorol. Climatol.* **52** 2051–64
Luo M and Lau N-C 2018 Increasing heat stress in urban areas of eastern China: acceleration by urbanization *Geophys. Res. Lett.* **45** 13060–9
Marchin R M, Backes D, Ossola A, Leishman M R, Tjoelker M G and Ellsworth D S 2022 Extreme heat increases stomatal conductance and drought-induced mortality risk in vulnerable plant species *Glob. Change Biol.* **28** 1133–46
Martínez-Ferrer L, Moreno-Martínez Á, Campos-Taberner M, García-Haro F J, Muñoz-Marí J, Running S W, Kimball J, Clinton N and Camps-Valls G 2022 Quantifying uncertainty in high resolution biophysical variable retrieval with machine learning *Remote Sens. Environ.* **280** 113199
Medlyn B E, Duursma R A, Eamus D, Ellsworth D S, Prentice I C, Barton C V M, Crous K Y, de Angelis P, Freeman M and Wingate L 2011 Reconciling the optimal and empirical approaches to modelling stomatal conductance *Glob. Change Biol.* **17** 2134–44
Meili N *et al* 2020 An urban ecohydrological model to quantify the effect of vegetation on urban climate and hydrology (UT&C v1.0) *Geosci. Model Dev.* **13** 335–62
Meili N, Manoli G, Burlando P, Carmeliet J, Chow W T L, Coutts A M, Roth M, Velasco E, Vivoni E R and Fatichi S 2021 Tree effects on urban microclimate: diurnal, seasonal, and climatic temperature differences explained by separating radiation, evapotranspiration, and roughness effects *Urban For. Urban Green.* **58** 126970
Mora C *et al* 2017 Global risk of deadly heat *Nat. Clim. Change* **7** 501–6
Moran M S, Clarke T R, Inoue Y and Vidal A 1994 Estimating crop water deficit using the relation between surface-air temperature and spectral vegetation index *Remote Sens. Environ.* **49** 246–63
Muller J D, Rotenberg E, Tatarinov F, Oz I and Yakir D 2021 Evidence for efficient nonevaporative leaf-to-air heat dissipation in a pine forest under drought conditions *New Phytol.* **232** 2254–66
O'sullivan O S *et al* 2017 Thermal limits of leaf metabolism across biomes *Glob. Change Biol.* **23** 209–23
Perkins-Kirkpatrick S E and Lewis S C 2020 Increasing trends in regional heatwaves *Nat. Commun.* **11** 3357
Rana G, de Lorenzi F, Mazza G, Martinelli N, Muschitiello C and Ferrara R M 2020 Tree transpiration in a multi-species Mediterranean garden *Agric. For. Meteorol.* **280** 107767
Richards D R, Belcher R N, Carrasco L R, Edwards P J, Fatichi S, Hamel P, Masoudi M, McDonnell M J, Peleg N and Stanley M C 2022 Global variation in contributions to human well-being from urban vegetation ecosystem services *One Earth* **5** 522–33
Skinner C B, Poulsen C J and Mankin J S 2018 Amplification of heat extremes by plant CO_2 physiological forcing *Nat. Commun.* **9** 1094
Speak A F, Rothwell J J, Lindley S J and Smith C L 2013 Reduction of the urban cooling effects of an intensive green roof due to vegetation damage *Urban Clim.* **3** 40–55
Teskey R, Wertin T, Bauweraerts I, Ameye M, Mcguire M A and Steppe K 2015 Responses of tree species to heat waves and extreme heat events *Plant Cell Environ.* **38** 1699–712
Venter Z S, Chakraborty T and Lee X 2021 Crowdsourced air temperatures contrast satellite measures of the urban heat island and its mechanisms *Sci. Adv.* **7** eabb9569
Wang C, Wang Z H, Wang C and Myint S W 2019 Environmental cooling provided by urban trees under extreme heat and cold waves in U.S. cities *Remote Sens. Environ.* **227** 28–43
Wong N H, Tan C L, Kolokotsa D D and Takebayashi H 2021 Greenery as a mitigation and adaptation strategy to urban heat *Nat. Rev. Earth Environ.* **2** 166–81
Wouters H, de Ridder K, Poelmans L, Willems P, Brouwers J, Hosseinzadehtalaei P, Tabari H, Vanden Broucke S, van Lipzig N P M and Demuzere M 2017 Heat stress increase under climate change twice as large in cities as in rural areas: a study for a densely populated midlatitude maritime region *Geophys. Res. Lett.* **44** 8997–9007
Yang J *et al* 2019 Incorporating non-stomatal limitation improves the performance of leaf and canopy models at high vapour pressure deficit *Tree Physiol.* **39** 1961–74
Yang L *et al* 2018 A new generation of the United States National Land Cover Database: requirements, research priorities, design, and implementation strategies *ISPRS J. Photogramm. Remote Sens.* **146** 108–23
Zander K K, Cadag J R, Escarcha J and Garnett S T 2018 Perceived heat stress increases with population density in urban Philippines *Environ. Res. Lett.* **13** 084009
Zhang G, He B-J and Dewancker B J 2020 The maintenance of prefabricated green roofs for preserving cooling performance: a field measurement in the subtropical city of Hangzhou, China *Sustain. Cities Soc.* **61** 102314
Zhang X, Liu L, Chen X, Gao Y, Xie S and Mi J 2021 GLC_FCS30: global land-cover product with fine classification system at 30 m using time-series Landsat imagery *Earth Syst. Sci. Data* **13** 2753–76